

# Simulating and Evaluating the Drilling of Carbon Fiber Reinforced Epoxy Material

[1] Suresh Aadepe, [2] Dr. Lachiram, [3] Dr. P. Ramesh Babu

[1] Research Scholar, Mechanical Department, O. U., [2] Mechanical Department, DLRL-Scientist-F, [3] Mechanical Department, Osmania University.

[1] adepuresh97@gmail.com, [2] lachiram@gmail.com, [3] prbmech@yahoo.com

---

**Abstract:** The use of composites in various industries, particularly the aerospace sector, has experienced a significant growth due to their exceptional mechanical properties. Drilling woven composite components is a common operation in assembly, making it essential to choose the optimal process parameters and tool geometry to avoid drilling-induced damage, such as delamination. This study introduces a new mathematical model to predict the critical thrust force at which delamination begins. The model considers the impact of thermo-mechanical loads and the mixed-mode fracture that occurs in the delamination zone for unidirectional composites. The proposed model has been compared to five previous models, encompassing various composite materials and feed rates, and was found to have the highest average accuracy. The study also includes a finite element analysis to visualize the phenomenon.

**Background:** The aerospace and automotive industries often require drilling holes in their material components during assembly. Annually, 250 million twist drill bits are used in the US aerospace industry and it is estimated that 55,000 holes are drilled for just one Airbus A350 unit. The problem with drilled holes in composite plates is that they are susceptible to damage. Previous research has shown that parts with drilled holes can result in a 30% decrease in fracture strength. Although molded holes are preferred, drilling is often necessary to attain the necessary positional and size tolerances.

**Materials and Methods:** The behavior of delamination prediction was visualized through the use of Finite Element Analysis. The process of drilling composite material was simulated in the following steps depicted in Figure 5. The drilling model consisted of three elements: a fluted drill bit, a UDT300/LTM45-EL laminate, and a backing plate and simulation setup was described

**Results:** To minimize delamination, the thrust force should be kept as low as possible. In conclusion, the frequency of fiber pull-out at the exit region of the drilled hole increased for the 45° fiber orientation compared to the restricted fiber orientations 30° and 60°.

**Conclusion:** Thrust force was found to have the greatest impact on damage in the composite when the thrust force exceeds the yield strength of the composite, delamination initiates. The delamination at the drill exit was always higher than at the drill entry. To minimize delamination, the thrust force should be kept as low as possible. In conclusion, the frequency of fiber pull-out at the exit region of the drilled hole increased for the 45° fiber orientation compared to the restricted fiber orientations 30° and 60°.

**Key Word:** Delamination, feed rate, drilling, critical thrust force, torque.

---

Date of Submission: 11-02-2023

Date of Acceptance: 22-02-2023

---

## I. Introduction

The aerospace and automotive industries often require drilling holes in their material components during assembly. Annually, 250 million twist drill bits are used in the US aerospace industry and it is estimated that 55,000 holes are drilled for just one Airbus A350 unit. The problem with drilled holes in composite plates is that they are susceptible to damage. Previous research has shown that parts with drilled holes can result in a 30% decrease in fracture strength. Although molded holes are preferred, drilling is often necessary to attain the necessary positional and size tolerances.

Contrary to the cutting mechanism in ductile metals, CFRPs (Carbon Fiber Reinforced Plastics) are dominated by a brittle crack propagation. The high thrust force from the drill can cause delamination of the plies in CFRPs due to the peel-up and push-out effect on the workpiece. To prevent delamination, the critical thrust force causing it must be identified and the feed rate should be adjusted accordingly. Tool wear adds to the complexity of the drilling process and requires the use of coolants, tool life monitoring, and effective drill design geometry.

Modeling the multilayer material machining process is complex and involves various factors such as material modeling, contact, fracture criteria, adaptive meshing, element types, and tool modeling. Previous

research has studied the drilling of CFRPs and concluded that drill geometry and feed rate are the most critical factors affecting the process. Additionally, the effect of fibre angle, cutting edge rounding, and elastic modulus on the drilling process have been investigated.

The objective of this work is to improve the development of a FE (Finite Element) drilling model that can accurately test various drill geometries with reasonable computation time. The FE model will be validated through experimental work investigating the effect of drilling forces and hole quality.

## II. Material And Methods

The behavior of delamination prediction was visualized through the use of Finite Element Analysis. The process of drilling composite material was simulated in the following steps depicted in Figure 5. The drilling model consisted of three elements: a fluted drill bit, a UDT300/LTM45-EL laminate, and a backing plate, as shown in Figure 6. The simulation setup was described in detail and exactly replicated as in Phadnis et al. [17].

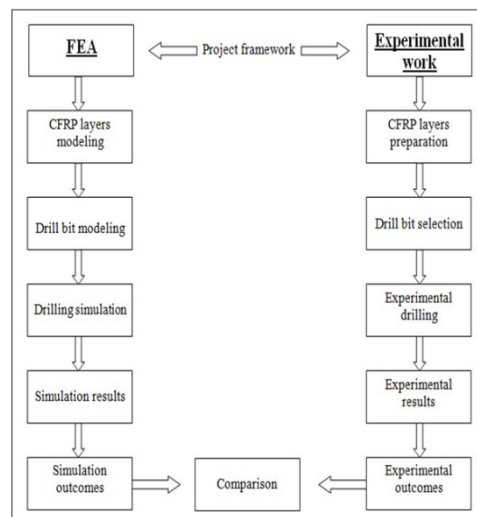


Fig 5: Flow Chart

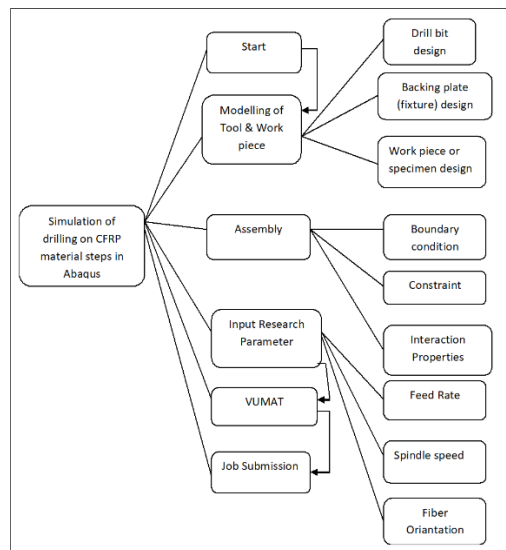


Fig 6: Process Flow (ABAQUS, Dassault Systems ®)

### A. Material Modelling

The composite material used in the model was a 70% fiber content orthotropic homogeneous Unidirectional (UD) epoxy/carbon fiber laminate T300/LTM45-EL. The mechanical and material properties of T300/LTM45-EL were obtained from the literature, as demonstrated by Phadnis et al. [17]. A custom-made 3D damage model, implemented as a VUMAT subroutine with solid elements, was created based on the properties of T300/LTM45-EL and integrated into the FE code ABAQUS/EXPLICIT (Dassault Systems®) to predict the

damage behavior and extent across the laminate thickness. Property selection

The mechanical properties of the plate material were considered as constant in the VUMAT subroutine to implement the 3D failure criteria. The tool and the composite plate were both modeled as solid homogenous sections and included in the module. The material orientation was considered based on the lay-up, with the most common orientations being (30°, 45°, 60°).

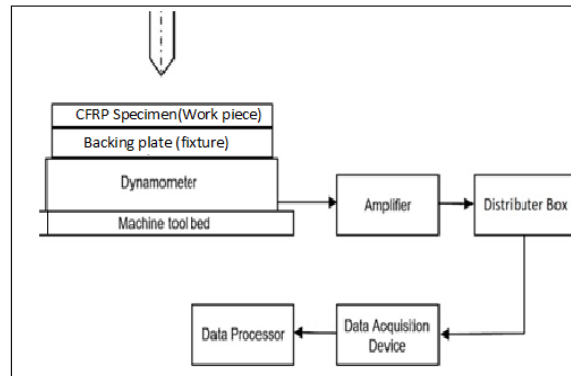


Figure 7: Schematic view of the composite drilling setup

### B. Delamination area and factor

The delamination area of a unidirectional laminate can be estimated by considering the principal directions as parallel and perpendicular to the fibers. A circular area can be assumed for the layer that the drill bit first encounters, and its diameter in the direction of the fibers will expand as the drill bit moves closer to the exit.

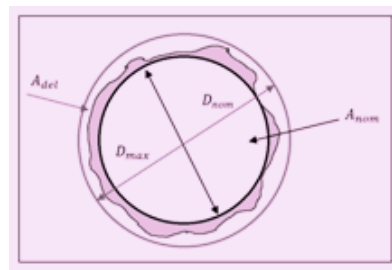


Figure 8: Delamination areas

The delamination factor,  $F_d$ , will be determined by using Eq. with  $d_{max}$  and  $d$  representing the maximum diameter of delamination and the nominal diameter respectively [18].

### Numerical Modelling for drilling Composites

The use of Carbon Fiber Reinforced Polymers (CFRP) has risen in popularity in the aerospace industry due to their excellent fatigue resistance and impressive characteristics such as high strength-to-weight ratio and stiffness. These composites are usually manufactured through primary processes and require additional machining, such as drilling, for assembly purposes. However, drilling composites can be more complex compared to drilling metals.

To overcome this challenge, numerical simulation has become more widespread in recent years due to advancements in computing power and the development of new simulation methods. The aim of this research is to study the impact of drill bit geometric parameters, such as chisel edge width, helix angle, and point angle, on delamination.

Finite Element Analysis (FEA) has proven to be a valuable tool in determining the parameters affecting the drilling process and providing accurate predictions. It can minimize experimental expenses and increase efficiency. FEA has been used to model material removal in orthogonal cutting and fracture in carbon fiber reinforced materials by various authors.

This study aims to evaluate the effect of orientation on delamination during drilling by using a 3D model simulation to visualize the growth of the delaminated area. The research focuses on the suitable material properties, failure criteria, and workpiece characteristics required for an accurate simulation of delamination in drilling.

Meshing

The parts formed in Abaqus/CAE are meshed using different mesh control approaches to meet the needs of the analysis. There are three common mesh designs in Abaqus: Eulerian, Lagrangian, and Arbitrary Lagrangian-Eulerian [29]. The table below outlines the differences between these methods. The simulation uses Eight-node brick elements with reduced-Integration (C3D8R) for unidirectional carbon fiber reinforced composites and COH3D8 type elements for cohesive zone elements. To achieve more accurate results, the mesh in the damaged area around the drilled hole is refined by a factor of three. The solution convergence is influenced by the element size, with a balance typically sought between element size and convergence without compromising the accuracy of the simulation [30]. The drill bit has the same element size as the plate and its elements are designated as rigid with respect to a reference point, usually the drill bit tip. A rigid body is modeled with elements set with displacement directed relative to a reference node, with the relative distances between nodes remaining constant and non-deforming throughout the simulation.

C. Boundary conditions

All the boundary conditions for the drill bits with The boundary conditions for the drill bits, including the velocity boundary condition, feed rate, and spindle speed, are applied to the reference point in the z-direction. The CFRP composite plate is modeled as clamped with its vertical edges fixed. Figure 9 shows the setup.

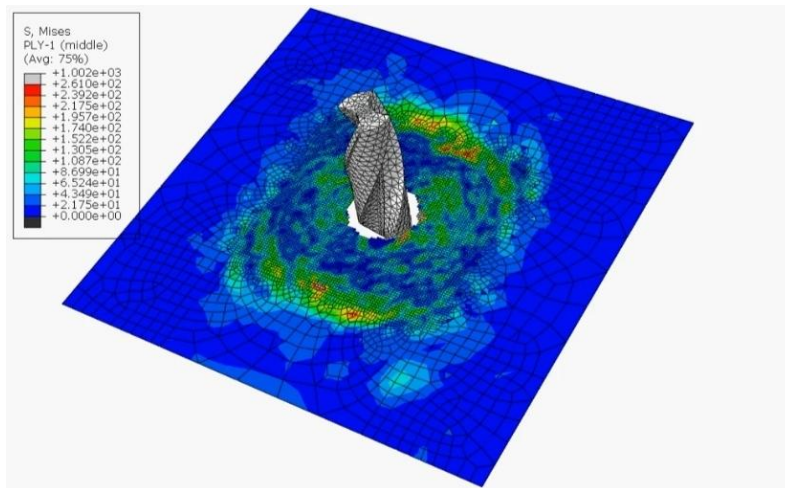


Figure 9: Drilling of CFRP material

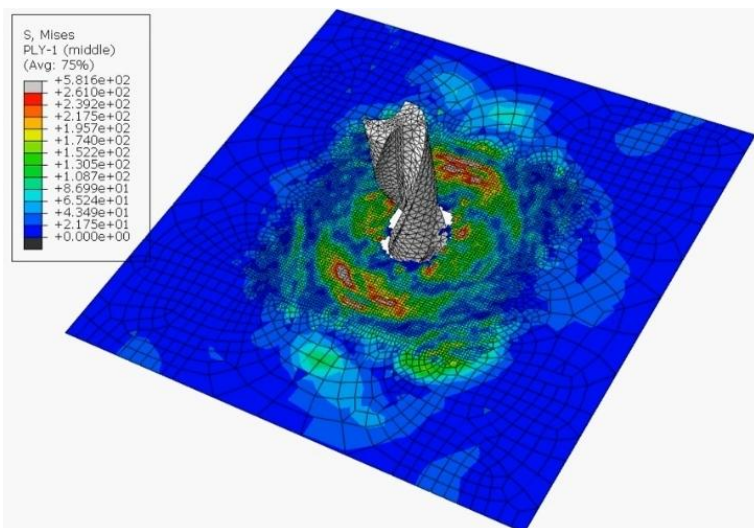


Figure 10: Simulation set up

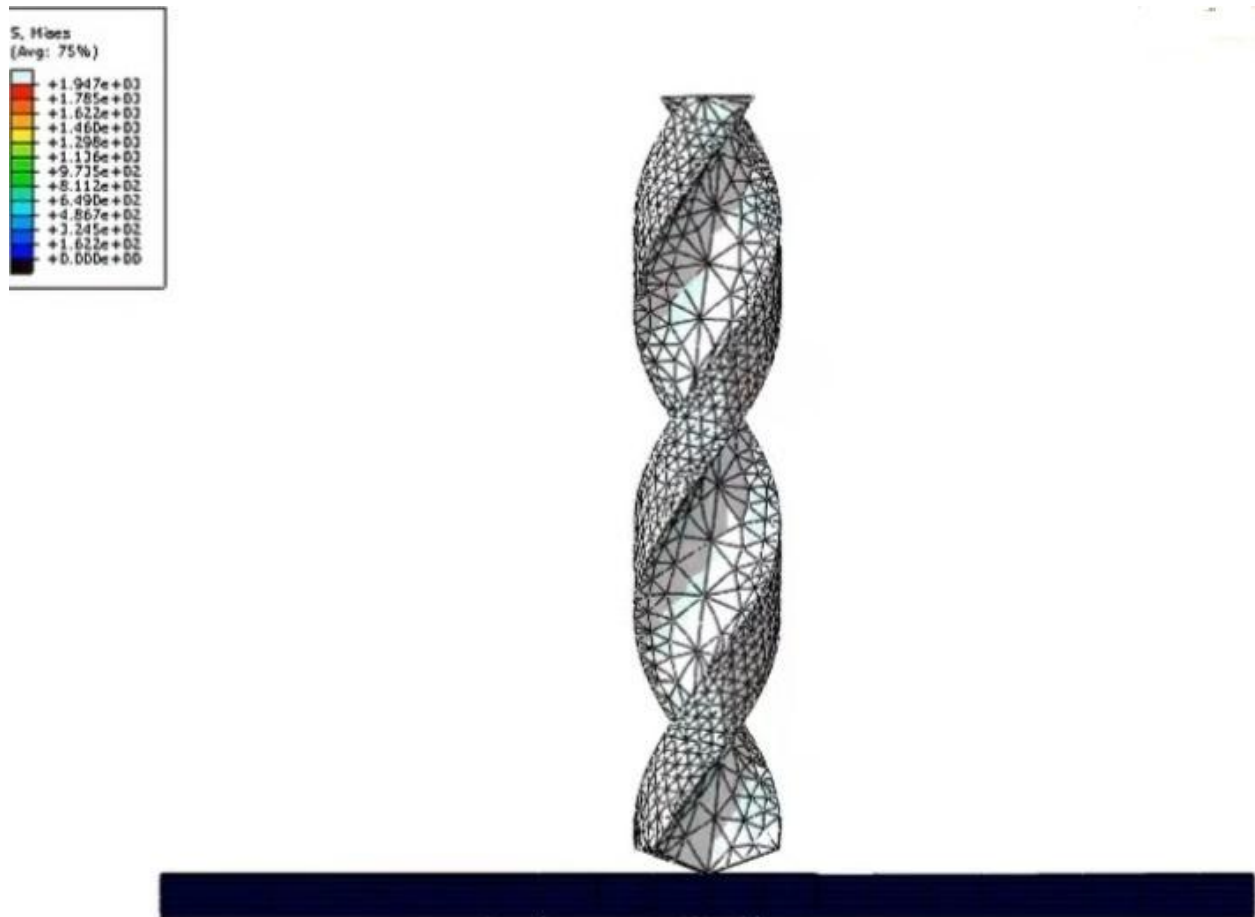


Figure 11: Simulation process

## II. RESULTS AND DISCUSSIONS

To make a more informed comparison of the impact of various orientations on drilling CFRP, three feed rates (100 mm/min, 150 mm/min, and 200 mm/min) were selected from experimental data for orientations [30°, 45°, 60°] reported by Phadnis et al. [18]. The feed rate was kept constant at 2500 rpm, and the finite element simulations were carried out using these process parameters. The results of these simulations were then used to validate and predict the thrust force, torque, and delamination factor for other feed rates in various orientation sequences.

### Validation of Finite Element model

The percentage of error between the experimental data and simulation data, as shown in Table 1, indicates that the highest percentage error for thrust force was 13.5% at a feed rate of 100 mm/s, while the highest percentage error for torque was 11.08% at a feed rate of 100 mm/s.

Table 1. Summary of percentage error for thrust force and torque [32]

| Speed Rpm | Feed rate (mm/min) | Thrust force (N) |        |                      | Torque (N.mm) |       |                      |
|-----------|--------------------|------------------|--------|----------------------|---------------|-------|----------------------|
|           |                    | Experiment       | FEA    | Percentage error (%) | Experiment    | FEA   | Percentage error (%) |
| 1000      | 100                | 54               | 67.5   | 13.5                 | 370           | 411   | 11.08                |
| 1000      | 150                | 65               | 74.75  | 9.75                 | 400           | 430   | 7.50                 |
| 1000      | 200                | 93               | 106.02 | 10.02                | 355           | 365.2 | 10.2                 |
| 1200      | 100                | 63.5             | 76.2   | 12.7                 | 460           | 500   | 8.70                 |
| 1200      | 150                | 109              | 114.45 | 5.45                 | 557.75        | 600   | 7.58                 |
| 1200      | 200                | 53               | 65.5   | 12.5                 | 440           | 470   | 6.82                 |
| 1400      | 100                | 68               | 78.2   | 10.2                 | 287.5         | 300   | 4.35                 |
| 1400      | 150                | 129              | 135.45 | 6.45                 | 330           | 354   | 7.27                 |
| 1400      | 200                | 135              | 142.15 | 7.15                 | 295           | 320   | 8.47                 |

The comparison between the thrust force obtained from experiments and simulations is shown in Figure 12. It demonstrates that the thrust force from the experiments is 5.45% lower than that from the simulations. Figure 13 presents the comparison of torque between the experiment and simulations of [30°,45°,60°]. The torque from the experiments is also 4.35% lower than the torque from the simulations. These comparisons indicate that the FE model provides a good estimate for the thrust force and torque with a discrepancy less than 13% [31,32].

Several variables that were not physically modeled in the simulation, such as the effects of heat generation and drill wear, may have contributed to the difference. Additionally, the simulation used a constant coefficient of friction throughout, whereas the experiments used an average of a set of tests for the value, which may not be consistent. The lack of an accurate friction coefficient is a limitation in the FEA analysis. The material's properties and the type of elements used to represent the material may also impact the results. The default and simplified algorithm scheme available in Abaqus/Explicit may also have contributed to the differences due to mathematical solver simplification [33,34].

Graphs:

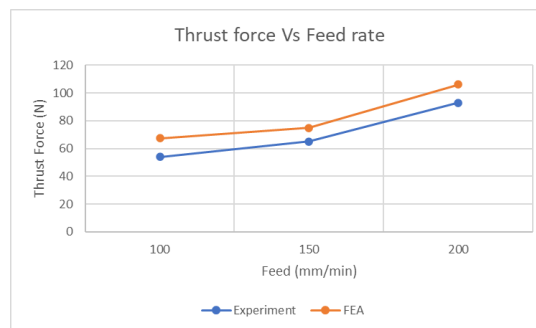


Fig 12: Comparison of thrust force between experiment and simulation for [30°,45°,60°]

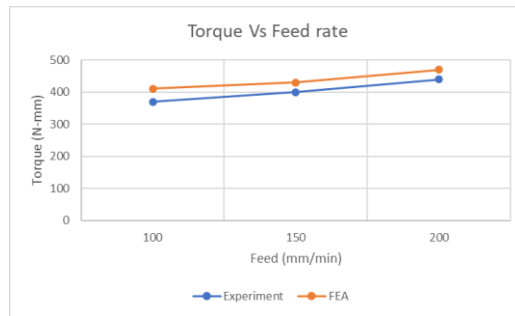


Figure 13: Comparison of torque between experiment and simulation for [30°,45°,60°]

### III. DELAMINATION

#### A. Measuring Delamination

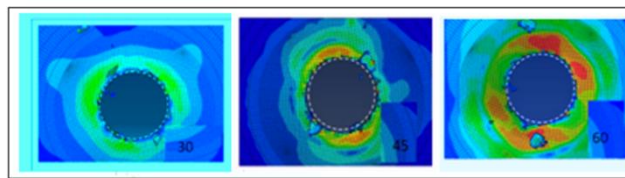


Figure 14: Entrance to exit (left to right) delaminated area with lay-up [20,27,30]

The delamination factor in this FE simulation was determined by computing the ratio of the total number and size of cohesive elements prior to and after the drilling simulation, using the simple methodology described in Eq. The corresponding delamination factors for drill entry and exit are presented in Table 2 for all orientation sequences. The orientation sequence [30°/45°/60°] resulted in the highest delamination factor, with a significant increase as the feed rate increased, compared to the orientation sequence that produced the lowest value.

Table 2. Summary of Experimental delamination factor in different orientations [32]

| Speed Rpm | Feed mm/min | Fiber Orientation (angle) | Thrust kN | Torque kN-mm | Fd(in)  | Fd(out) |
|-----------|-------------|---------------------------|-----------|--------------|---------|---------|
| 1         | 1000        | 100                       | 30        | 0.054        | 0.37    | 1.068   |
| 2         | 1000        | 100                       | 45        | 0.0525       | 0.5105  | 1.327   |
| 3         | 1000        | 100                       | 60        | 0.059        | 0.4475  | 1.553   |
| 4         | 1000        | 150                       | 30        | 0.051        | 0.28    | 1.054   |
| 5         | 1000        | 150                       | 45        | 0.065        | 0.4     | 1.315   |
| 6         | 1000        | 150                       | 60        | 0.066        | 0.22    | 1.523   |
| 7         | 1000        | 200                       | 30        | 0.049        | 0.26    | 1.049   |
| 8         | 1000        | 200                       | 45        | 0.424        | 0.31    | 1.305   |
| 9         | 1000        | 200                       | 60        | 0.093        | 0.355   | 1.558   |
| 10        | 1200        | 100                       | 30        | 0.056        | 1.02    | 1.065   |
| 11        | 1200        | 100                       | 45        | 0.0635       | 0.46    | 1.328   |
| 12        | 1200        | 100                       | 60        | 0.139        | 0.425   | 1.549   |
| 13        | 1200        | 150                       | 30        | 0.062        | 0.46    | 1.065   |
| 14        | 1200        | 150                       | 45        | 0.104        | 0.37    | 1.288   |
| 15        | 1200        | 150                       | 60        | 0.109        | 0.55775 | 1.562   |
| 16        | 1200        | 200                       | 30        | 0.053        | 0.44    | 1.078   |
| 17        | 1200        | 200                       | 45        | 0.0785       | 0.18    | 1.312   |
| 18        | 1200        | 200                       | 60        | 0.087        | 0.8475  | 1.545   |
| 19        | 1400        | 100                       | 30        | 0.035        | 0.61    | 1.08    |
| 20        | 1400        | 100                       | 45        | 0.059        | 0.28    | 1.318   |
| 21        | 1400        | 100                       | 60        | 0.068        | 0.2875  | 1.557   |
| 22        | 1400        | 150                       | 30        | 0.129        | 0.33    | 1.055   |
| 23        | 1400        | 150                       | 45        | 0.08         | 0.395   | 1.285   |
| 24        | 1400        | 150                       | 60        | 0.071        | 0.295   | 1.552   |
| 25        | 1400        | 200                       | 30        | 0.19         | 0.38    | 1.058   |

|    |      |     |    |       |        |       |
|----|------|-----|----|-------|--------|-------|
| 26 | 1400 | 200 | 45 | 0.135 | 0.295  | 1.305 |
| 27 | 1400 | 200 | 60 | 0.073 | 1.0125 | 1.565 |

The results indicated that a higher feed rate led to an increased thrust force on the surface of the composite material. The highest damaged area and thrust force were observed at a feed rate of 200 mm/min, which produced a force of 135 N, while the thrust forces at feed rates of 150 mm/min and 100 mm/min were 129 N and 68 N, respectively, as depicted in Figure 8, which shows the damaged area and thrust produced for different feed rates in a 2D and 3D view of the composite laminate workpiece over a total drilling time of 1.2 seconds.

It was observed that the delamination factor was higher at the drill entry than at the drill exit, as expected. For the orientation sequence of  $[60^\circ]$  at a feed rate of 150 mm/min, the delamination factor at the entry was 1.562 and at the exit was 1.2905. The percentage of the delamination factor decreased as the feed rate increased. The highest delamination factor indicated a greater amount of damage. Thus, it can be concluded that choosing a suitable feed rate is crucial in reducing damage to the composite material. In practical terms, the feed rate should be kept as low as possible to minimize damage extension. Delamination occurs in composite materials when the thrust force acting on the composite is greater than the composite's yield strength, and the cohesive elements in the composite play an important role in delamination. Additionally, the ratio of the chisel edge force to the total thrust force was investigated, and the question of how the width of the chisel edge affects the chisel edge ratio,  $\gamma$ , was considered.

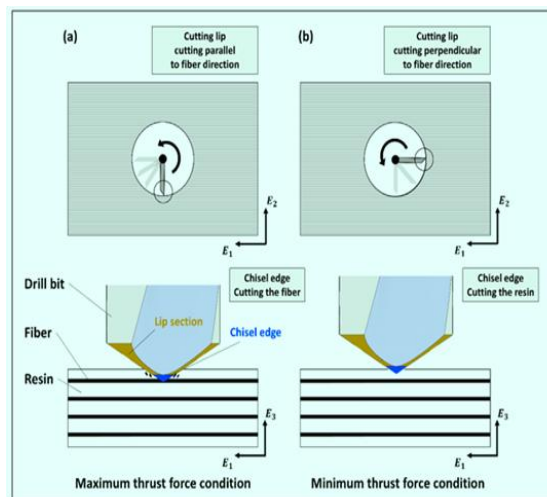


Figure 14: Force fluctuation mechanisms. (a) The maximum force occurs when the angle between the cutting lip and fiber is  $(\theta^0 = 45^\circ)$ , and (b) the minimum thrust force occurs when the angle between the cutting lip and fiber is  $60^\circ$  ( $\theta^0 = 30^\circ$ ).



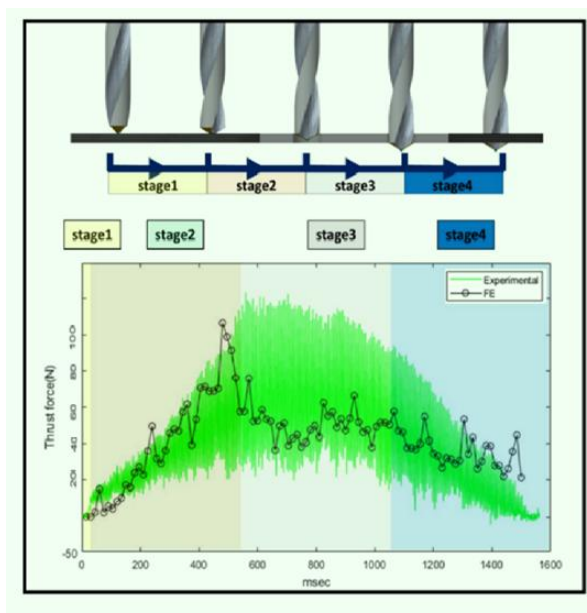


Figure 15: FE model setup for (a) Drill bit (b) Isometric view (c) Radial view with dimensions (d) boundary condition with half section view (e) ply stacking sequence with the cohesive surfaces.

### III. Conclusion

In this paper, the impact of various machining parameters on the thrust force and drilling torque for UD-T300/LTM45-EL composite laminate was analyzed both numerically and experimentally validated using published data for  $[30^\circ/45^\circ/60^\circ]$ . The material behavior was modeled as an orthotropic response, incorporating a thrust-based damage criterion using a VUMAT subroutine in ABAQUS/EXPLICIT. The element deletion method, based on threshold thrust levels in carbon fiber and epoxy matrix materials, was implemented to simulate the hole-making process in drilling.

The results showed that the thrust force is directly proportional to the feed rate, with a difference of 4.35% between the computational model and the experiment. Among the orientation sequences, the highest thrust force was observed at 200 mm/min and 150 mm/min feed rates, with values of 0.135 kN and 0.557 kN.mm, respectively. Delamination extent increased as the frequency of fiber pull-out at the exit region of the drilled hole increased for the  $45^\circ$  fiber orientation, compared to the restricted fiber orientations  $30^\circ$  and  $60^\circ$ .

Thrust force was found to have the greatest impact on damage in the composite. When the thrust force exceeds the yield strength of the composite, delamination initiates. The delamination at the drill exit was always higher than at the drill entry. To minimize delamination, the thrust force should be kept as low as possible. In conclusion, the frequency of fiber pull-out at the exit region of the drilled hole increased for the  $45^\circ$  fiber orientation compared to the restricted fiber orientations  $30^\circ$  and  $60^\circ$ .

### References

- [1]. DeGarmo, E.; Black, J.; Kohser, R. *Materials and Processes in Manufacturing*; Wiley: Hoboken, NJ, USA, 2003.
- [2]. Faraz, A.; Biermann, D.; Weinert, K. Cutting edge rounding: An innovative tool wear criterion in drilling CFRP composite laminates. *Int. J. Mach. Tools Manuf.* 2009, 49, 1185–1196. [CrossRef]
- [3]. Zitoune, R.; Crouzeix, L.; Collombet, F.; Tamine, T.; Grunevald, Y. Behaviour of composite plates with drilled and moulded hole under tensile load. *Compos. Struct.* 2011, 93, 2384–2391. [CrossRef]
- [4]. Karata, S., M.A.; Gökçaya, H. A review on machinability of carbon fiber reinforced polymer (CFRP) and glass fiber reinforced polymer (GFRP) composite materials. *Def. Technol.* 2018, 14, 318–326, *Composite Materials in Defence Technology*. [CrossRef]
- [5]. Wang, H.; Zhang, H.; Goto, K.; Watanabe, I.; Kitazawa, H.; Kawai, M.; Mamiya, H.; Fujita, D. Thrust mapping reveals extrinsic toughening of brittle carbon fiber in polymer matrix. *Sci. Technol. Adv. Mater.* 2020, 21, 267–277. [CrossRef]
- [6]. König, W.; Wulf, C.; Grass, P.; Willerscheid, H. *Machining of Fibre Reinforced Plastics*. *CIRP Ann.* 1985, 34, 537–548. [CrossRef]
- [7]. Ismail, S.O.; Sarfraz, S.; Niamat, M.; Mia, M.; Gupta, M.K.; Pimenov, D.Y.; Shehab, E., *Comprehensive Study on Tool Wear During Machining of Fiber-Reinforced Polymeric Composites*. In *Machining and Machinability of Fiber Reinforced Polymer Composites*; Hameed Sultan, M.T., Azmi, A.I., Majid, M.S.A., Jamir, M.R.M., Saba, N., Eds.; Springer: Singapore, 2021; pp. 129–147. [CrossRef]
- [8]. Vijayaraghavan, A.; Dornfeld, D. *Challenges in Modelling Machining of Multilayer Materials*, 2005. Available online: <https://escholarship.org/uc/item/60k6x64r#author> (accessed on 10 January 2018).
- [9]. Panchagnula, K.K.; Palaniyandi, K. Drilling on fiber reinforced polymer/nanopolymer composite laminates: A review. *J. Mater. Res. Technol.* 2018, 7, 180–189. [CrossRef]
- [10]. Lissek, F.; Tegas, J.; Kaufeld, M. Damage Quantification for the Machining of CFRP: An Introduction about Characteristic Values Considering Shape and Orientation of Drilling-induced Delamination. In *Proceedings of the International Conference on Manufacturing Engineering and Materials, ICMEM 2016, Nový Smokovec, Slovakia, 6–10 June 2016*; [CrossRef]

- [11]. Kahwash, F.; Shyha, I.; Maheri, A. Modelling of cutting fibrous composite materials: Current practice. *Procedia CIRP* 2015, 28, 52–57. [CrossRef]
- [12]. Liu, D.; Tang, Y.; Cong, W. A review of mechanical drilling for composite laminates. *Compos. Struct.* 2012, 94, 1265–1279. [CrossRef]
- [13]. Mahdi, M.; Zhang, L. A finite element model for the orthogonal cutting of fiber-reinforced composite materials. *J. Mater. Process. Technol.* 2001, 113, 373–377. [CrossRef]
- [14]. Shyha, I.; Aspinwall, D.; Soo, S.; Bradley, S. Drill geometry and operating effects when cutting small diameter holes in CFRP. *Int. J. Mach. Tools Manuf.* 2009, 49, 1008–1014. [CrossRef]
- [15]. Hale, P.; gene Ng, E. Non-linear material characterization of CFRP with FEM utilizing cohesive surface considerations validated with effective tensile test fixturing. *Mater. Today Commun.* 2020, 23, 100872. [CrossRef]
- [16]. Hale, P.; Ng, E.G. Three-point bending analysis with cohesive surface interaction for improved delamination prediction and application of carbon fibre reinforced plastics composites. *Model. Simul. Mater. Sci. Eng.* 2020, 28, 035007. [CrossRef]
- [17]. V. A. Phadnis, F. Makhdum, A. Roy, and V. V. Silberschmidt, “Drilling in carbon/epoxy composites: Experimental investigations and finite element implementation,” *Compos. Part A Appl. Sci. Manuf.*, vol. 47, no. 1, pp. 41–51, Apr. 2013, doi: 10.1016/j.compositesa.2012.11.020.
- [18]. V. N. Gaitonde, S. R. Karnik, J. C. Rubio, A. E. Correia, A. M. Abrão, and J. P. Davim, “Analysis of parametric influence on delamination in high-speed drilling of carbon fiber reinforced plastic composites,” *J. Mater. Process. Technol.*, vol. 203, no. 1–3, pp. 431–438, Jul. 2008, doi: 10.1016/j.jmatprotec.2007.10.050.
- [19]. Singh, I. N. Bhatnagar, and P. Viswanath, Drilling of uni-directional glass fiber reinforced plastics: experimental and finite element study. *Materials & Design*, 2008, 29(2): p. 546-553.
- [20]. Phadnis, V.A., F. Makhdum, A. Roy, and V.V. Silberschmidt, Drilling in carbon/epoxy composites: experimental investigations and finite element implementation. *Composites Part A: Applied Science and Manufacturing*, 2013, 47: p. 41-51.
- [21]. Durão, L., M. De Moura, and A. Marques, Numerical prediction of delamination onset in carbon/epoxy composites drilling. *Engineering Fracture Mechanics*, 2008, 75(9): p. 2767-2778.
- [22]. Khanna, N., F. Pusavec, C. Agrawal, and G.M. Krolczyk, Measurement and evaluation of hole attributes for drilling CFRP composites using an indigenously developed cryogenic machining facility. *Measurement*, 2020, 154: p. 107504.
- [23]. Upputuri, H.B., V.S. Nimmagadda, and E. Duraisamy, Optimization of drilling parameters on carbon fiber reinforced polymer composites using fuzzy logic. *Materials Today: Proceedings*, 2020, 23: p. 528-535.
- [24]. Suresh Aadepe, Literature of Optimized Machining of Carbon Fiber Epoxy Composites Material Published In JETIR, ISSN :63975, Volume 6 Issue 2, February-2019.
- [25]. Suresh Aadepe, The Scientific Procedure of Research Work for Machining CFRP Material, Volume 6, Issue: 1, February 2019.
- [26]. Wang, D., X. He, Z. Xu, W. Jiao, F. Yang, L. Jiang, L. Li, W. Liu, and R. Wang, Study on damage evaluation and machinability of UD-CFRP for the orthogonal cutting operation using scanning acoustic microscopy and the finite element method. *Materials*, 2017, 10(2): p. 204.
- [27]. Van Luttervelt, C., T. Childs, I. Jawahir, F. Klocke, P. Venuvinod, Y. Altintas, E. Armarego, D. Dornfeld, I. Grabec, and J. Leopold, Present situation and future trends in modelling of machining operations progress report of the CIRP Working Group ‘Modelling of Machining Operations’. *CIRP Annals*, 1998, 47(2): p. 587-626.
- [28]. Mahdi, M. and L. Zhang, A finite element model for the orthogonal cutting of fiber-reinforced composite materials. *Journal of materials processing technology*, 2001, 113(1-3): p. 373-377.
- [29]. Dandekar, C.R. and Y.C. Shin, Modeling of machining of composite materials: a review. *International Journal of Machine tools and manufacture*, 2012, 57: p. 102-121.
- [30]. Wang, G.-D. and S.K. Melly, Three-dimensional finite element modeling of drilling CFRP composites using Abaqus/CAE: a review. *The International Journal of Advanced Manufacturing Technology*, 2018, 94(1): p. 599-614.
- [31]. Suresh Aadepe, Experimental Investigation on Influence of Process Parameters and Drilling Performance Optimization journal of North Eastern University Volume 25 Issue 04, 2022 ISSN: 1005-3026.
- [32]. [32] O. Isbilir and E. Ghassemieh, “Finite element analysis of drilling of titanium alloy,” in *Procedia Engineering*, Jan. 2011, vol. 10, pp. 1877–1882, doi: 10.1016/j.proeng.2011.04.312.
- [33]. Ullah, H., A.R. Harland, T. Lucas, D. Price, and V.V. Silberschmidt, Finite- element modelling of bending of CFRP laminates: Multiple delaminations. *Computational Materials Science*, 2012, 52(1): p. 147-156.
- [34]. Boresi, A.P., R.J. Schmidt, and O.M. Sidebottom, *Advanced mechanics of materials*. Vol. 6. 1993: Wiley New York.
- [35]. Hashin, Z. and A. Rotem, A fatigue failure criterion for fiber reinforced materials. *Journal of composite materials*, 1973, 7(4): p. 448-464.
- [36]. Phadnis, V., A. Roy, and V. Silberschmidt. Finite element analysis of drilling in carbon fiber reinforced polymer composites. in *Journal of Physics- Conference Series*. 2012.

Fabio Pundo, et. al. “Comparative Analysis of the Effects of Wind Load on Tall Reinforced Concrete Buildings for Ordinary Use in Luanda According to ABNT and Eurocode.” *IOSR Journal of Mechanical and Civil Engineering (IOSR-JMCE)*, 20(1), 2023, pp. 01-10.